Fast approximators for optimal low-thrust hops between main belt asteroids

Daniel Hennes
Robotics Innovation Center
DFKI
Bremen, Germany
Email: daniel.hennes@dfki.de

Dario Izzo
Advanced Concepts Team
ESA, ESTEC
Noordwijk, The Netherlands
Email: dario.izzo@esa.int

Damon Landau
Jet Propulsion Laboratory
NASA
Pasadena, CA, United States
Email: damon.landau@jpl.nasa.gov

***Abstract*—We consider the problem of optimally transferring a spacecraft from a starting to a target asteroid. We introduce novel approximations for important quantities characterizing the optimal transfer in case of short transfer times (asteroid hops). We propose and study in detail approximations for the phasing value φ, for the maximum initial mass m^* and for the arrival mass m_f. The new approximations require orders of magnitude less computational effort with respect to state-of-the-art algorithms able to compute their ground-truth value. The accuracy of the introduced approximations is also found to be orders of magnitude superior with respect to other, commonly used, approximations based, for example, on Lambert models. Our results are obtained modelling the physics of the problem as well as employing computational intelligence techniques including the multi-objective evolutionary algorithm by decomposition framework, the hypervolume indicator and state of the art machine learning regressors.**

I. Introduction

In has become increasingly clear how the preliminary phases in the design of an interplanetary trajectory consider a search space often dominated by a vast combinatorial part as well as by a high dimensional continuous part. The combinatorial part is typically related to some choice (e.g. target body selection, selection of the propulsion system, fly-by sequence selection, target observation selection, etc.) while the continuous part stems from the problem of optimally controlling the spacecraft as to save resources such as time and propellant mass. The structure of the problem appears thus to be very much suitable for the application of computational intelligence (CI) techniques, and in particular of intelligent search methods. While studied also in this context, these techniques are still on their way to become established tools. A fact that is demonstrated, for example, by the limited attention CI methods receive during the international global trajectory competition (GTOCs) events [1], where many participants try some CI technique but end up not using it prominently (a notable exception being the HUMIES gold medal winner trajectory in 2014 [2]). One of the reasons for this difficulty, can be found in the specific structure of the interplanetary trajectory search domain and, in particular, in the complex continuous part of the search space which demands competences in astrodynamics and optimal control theory and typically absorbs a lot of computational resources. The ability to approximate the effect of the continuous choices and thus to be able to build good heuristics able to guide the search in the combinatorial part of the space is of great importance. Various approximations and closed form solutions to optimal low-thrust transfers have been proposed in the past, starting from Edelbaum's work [3] to shape methods [4], but in most situations they are either still computationally too costly or not informative enough to drive the combinatorial part of the search for preliminary designs. A often used and popular approximation to low-thrust transfers, is based on impulsive manoeuvres and, frequently, on two impulse transfers as they are computed very efficiently by solving Lambert's problem.

In this paper we propose three new approximators for the problem of optimal asteroid hops, here intended as the solution to the optimal control problems arising from a low-thrust transfer between asteroids subject to short transfer times (i.e. transfers not requiring multiple revolutions around the Sun). Our work is mainly motivated to refine search methods in multiple asteroid rendezvous problems such as the ones described in the 7th edition of the GTOC. However, the approximations and methods proposed are more general and could have relevance, for example, also for Near Earth Asteroid missions or debris removal missions.

II. The phasing value φ

A recurring problem in the design of interplanetary trajectories for multiple asteroid rendezvous missions is that of selecting and ranking transfer opportunities (target body, arrival epoch, arrival mass, etc.) presented to a spacecraft S co-orbiting some initial asteroid. Ideally, one would want to obtain this information without having to design an actual optimal transfer, as there could be tens of thousands of possible targets to consider and trying to design a transfer to each one of them for ranking purposes would be unpractical. A straight forward option is to preliminary rank the possible transfer options according to the orbital parameter differences between the source and target orbit or using some ideal approximation of the necessary ΔV (e.g. neglecting the relative phasing: the actual positions of the source and target asteroid along their orbit), to then focus only on the top ranked opportunities. This often results in pruning out good targets mis-ranked by these criteria. A good ranking criterion has to account for the orbital phasing, for the spacecraft propulsion system, for the available transfer time and has to be multi-objective as to consider fast transfers as well as low ΔV transfers as good outcomes. Recently, a formal definition of such a ranking criterion (the phasing value), based on the hypervolume of the non-dominated front obtained from a chemical representation

of the transfer, was given in [5]. In this work, a constraint based on a simplistic Lambert approximation was considered to make sure the chemical ΔV could be converted into a low-thrust ΔV. We here improve on this definition considering, instead, that constraint as $m_s < m^*$, where m_s is the starting mass of the spacecraft S and m^* is the maximum initial mass S can have in order for the transfer to be feasible in low-thrust. To approximate this quantity we use the Maximum Initial Mass Approximation (MIMA) m_D^* introduced in the second part of the paper (Eq.(8)) and shown to be vastly more accurate than the equivalent estimate based on a Lambert model.

A. Re-defining the phasing value

Consider, at t_0, a spacecraft S with mass m_s co-orbiting some asteroid $\mathcal{A}_1$ and a target asteroid $\mathcal{A}_2$. Let the starting (t_s) and final (t_f) epochs for a possible transfer $\mathcal{A}_1$-$\mathcal{A}_2$ vary freely in the window $[t_0, t_0 + \Delta T_M]$. Consider the following multi-objective optimization problem:

$$\begin{array}{rl} \text{find:} & t_s, t_f \in [t_0, t_0 + \Delta T_M] \\ \text{to minimize:} & f_1 = \Delta V, f_2 = t_f \\ \text{subject to:} & m_s \leq m_D^* \\ & t_s < t_f \end{array} \tag{1}$$

where ΔV is the sum of the two impulsive manoeuvres needed to match the velocities of the starting and arrival asteroid to that of the Lambert solution, the m_D^* is computed from the MIMA presented in Eq.(8) and $\Delta T = t_f - t_s$. A maximum thrust T_{max} and a specific impulse I_{sp} is assumed in the computation of m_D^*. Note how ΔT_M and ΔT may be different as well as t_0 and t_s. This constrained multi-objective problem can be solved by accounting for the constraints with a death penalty method [6] and solving the resulting unconstrained multi-objective problem by decomposition using, for example, MOEA/D [7] or PADE [8]. The resulting Pareto front is transformed into one number indicating its quality by computing its hypervolume [9] using as reference point $p^* = [\Delta T a_M/m_s, t_0 + \Delta T]$. The resulting number, called *phasing value* and denoted by $\varphi(\mathcal{A}_1, \mathcal{A}_2, t_0, \Delta T_M, m_s, T_{max}, I_{sp})$ (or $\varphi(\mathcal{A}_1, \mathcal{A}_2, t_0)$ in short) is measured in length units and captures the quality of the transfer opportunity $\mathcal{A}_1$-$\mathcal{A}_2$ in the window $[t_0, \Delta T_M]$ using a spacecraft S described by its starting mass m_s, the maximum thrust of its propulsion system T_{max} and its specific impulse I_{sp}. As an example, we show in Figure 1 the non dominated fronts in case $I_{sp} = 3000$ [s], $m_s = 1500$ [kg], $T_{max} = 0.3$ [N], $\Delta T_M = 365.25$ [days] and $t_0 = 11000$ [mjd2000] and corresponding to two specific hops from one asteroid $\mathcal{A}_1$ to two different targets in the main belt. The asteroid ids are referred to the main belt asteroids used during the GTOC7 competition [10]. The resulting hypervolumes are $h_1 = 0.61$ [AU] and $h_2 = 0.95$ [AU] indicating the asteroid with id. 3418 being better phased and thus representing a better target for a hop from a purely dynamical point of view.

B. Phasing indicators

The computation of the phasing value φ requires solving a two-dimensional, two-objectives problem and the computation of the final hypervolume. While a full analysis of the complexity of this task is beyond the scope of this paper, it maybe useful to report that in our reference architecture Intel(R) Core(TM) i7-4600U CPU @ 2.10GHz the implementation of

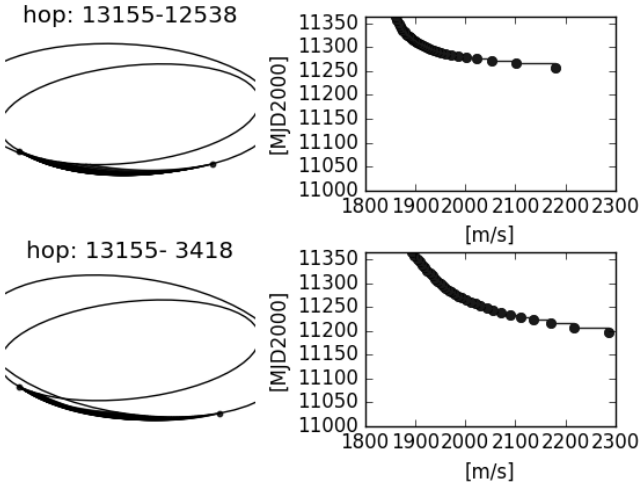

Fig. 1. Non dominated fronts representing the phasing value for two different target asteroids. This figure is equivalent to the corresponding plot in [5], but uses the updated definition of phasing value.

the above procedure takes roughly 120ms of CPU time when 32 distinct points are used to approximate the Pareto front. In a scenario were, say, thousands of asteroid hops have to be ranked this approach is unpractical. An improvement is obtained using the so-called *phasing indicators* introduced in [5] and allowing to rank transfer opportunities in a much shorter time while correlating well to the ground truth ranks produced by φ. We here discuss briefly the two indicators proposed in [5] (the Euclidean and the orbital) and introduce a new indicator having a superior rank correlation to the ground truth.

The *Euclidean indicator* $d_e(\mathcal{A}_1, \mathcal{A}_2, t_0)$ is defined in [5] as $d_e = |\mathbf{x}_2 - \mathbf{x}_1|$, where:

$$\mathbf{x} = [\mathbf{r}(t_0), \mathbf{v}(t_0)]$$

It contains information on both the asteroid relative positions and their relative velocities. The underlying idea is that asteroids physically near to each other (and having a small relative velocity) are likely to be good candidates for an orbital transfer, thus a low d_e is to be expected. The euclidean distance indicator can equivalently be written as $d_e = \sqrt{|\Delta\mathbf{r}|^2 + |\Delta\mathbf{v}|^2}$ where $\Delta\mathbf{r}$ and $\Delta\mathbf{v}$ are the differences between the asteroid ephemerides. The main drawback of this indicator is that it is unable to distinguish between a case where the relative velocity eventually brings the asteroids closer and a case (e.g. having an identical $|\mathbf{x}_2 - \mathbf{x}_1|$) where the relative velocity tends to separate the asteroids. Also, such an euclidean indicator, weights implicitly the difference in positions and velocities thus hiding the additional parameter $\gamma = 1$ [sec^2] that appears in its definition as $d_e = \sqrt{|\Delta\mathbf{r}|^2 + \gamma|\Delta\mathbf{v}|^2}$.

The *orbital indicator* $d_o(\mathcal{A}_1, \mathcal{A}_2, t_0, \Delta T)$ is defined in [5] as $d_o = |\mathbf{x}_2 - \mathbf{x}_1|$, where

$$\mathbf{x} = \left[\frac{1}{\Delta T}\mathbf{r}(t_0) + \mathbf{v}(t_0), \frac{1}{\Delta T}\mathbf{r}(t_0)\right]$$

It may be also be written as: $d_o = \sqrt{|\Delta\mathbf{V}_1|^2 + |\Delta\mathbf{V}_2|^2}$ where:

$$\begin{array}{l} \Delta\mathbf{V}_1 = \frac{1}{\Delta T}\Delta\mathbf{r} + \Delta\mathbf{v} \\ \Delta\mathbf{V}_2 = \frac{1}{\Delta T}\Delta\mathbf{r} \end{array} \tag{2}$$

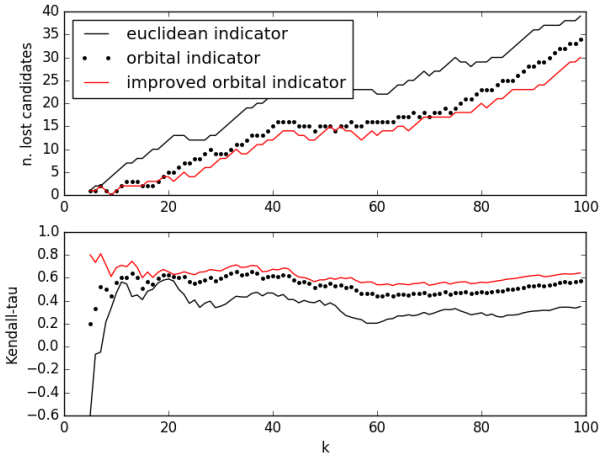

Fig. 2. The improved orbital indicator outperforms the others. Simulation averaging 100 different starting epochs and asteroids

and derives from a simple model of an orbital transfer neglecting entirely gravity. In this model $\mathcal{A}_1$ and $\mathcal{A}_2$ are assumed in a uniform rectilinear motion as well as the spacecraft S:

$$\begin{aligned}\mathbf{r}_1 &= \mathbf{r}_{10} + \mathbf{v}_{10}t \\ \mathbf{r}_2 &= \mathbf{r}_{20} + \mathbf{v}_{20}t \\ \mathbf{r}_S &= \mathbf{r}_{10} + \mathbf{v}_{S0}t\end{aligned}$$

Assuming to fix the transfer time to ΔT, we can match the final position of the spacecraft to that of the target asteroid obtaining: $\mathbf{v}_{S0} = \frac{\mathbf{r}_{20}-\mathbf{r}_{10}}{\Delta T} + \mathbf{v}_{20}$. Hence we may compute the velocity difference at t_0 between the spacecraft and the starting asteroid as $\frac{1}{\Delta T}\Delta\mathbf{r} + \Delta\mathbf{v}$ and the one between the spacecraft and the target asteroid at $t_0 + \Delta T$ as: $\frac{1}{\Delta T}\Delta\mathbf{r}$.

The *improved orbital indicator* $d_{o'}(\mathcal{A}_1, \mathcal{A}_2, t_0, \Delta T)$ is here defined as: $d_{o'} = |\mathbf{x}_2 - \mathbf{x}_1|$, where:

$$\mathbf{x} = \left[\frac{1}{\Delta T}\mathbf{r}(t_0) + \mathbf{v}(t_0), \frac{1}{\Delta T}\mathbf{r}(t_0), \right. \\ \left. \frac{1}{\Delta T}\mathbf{r}(t_0 + \Delta T) - \mathbf{v}(t_0 + \Delta T), \frac{1}{\Delta T}\mathbf{r}(t_0 + \Delta T)\right]$$

It is based on the same idea behind the *orbital indicator* d_o, but it tries to correct for the oversimplified linear dynamics by looking also at the differences in positions and velocities of the asteroids at $t_0 + \Delta T$. It does so, considering the backward-in-time transfer from $\mathcal{A}_2$ to $\mathcal{A}_1$ starting from $t_0 + \Delta T$ and modelled using the same linear model described above. Its definition can also be written as:

$$d_{o'} = \sqrt{|\Delta\mathbf{V}_1|^2 + |\Delta\mathbf{V}_2|^2 + |\Delta\mathbf{V}'_1|^2 + |\Delta\mathbf{V}'_2|^2}$$

where:

$$\begin{aligned}\Delta\mathbf{V}_1 &= \tfrac{1}{\Delta T}\Delta\mathbf{r} + \Delta\mathbf{v} \\ \Delta\mathbf{V}_2 &= \tfrac{1}{\Delta T}\Delta\mathbf{r} \\ \Delta\mathbf{V}'_1 &= \tfrac{1}{\Delta T}\Delta\mathbf{r}' - \Delta\mathbf{v}' \\ \Delta\mathbf{V}'_2 &= \tfrac{1}{\Delta T}\Delta\mathbf{r}'\end{aligned} \tag{3}$$

having indicated with $\Delta\mathbf{r}'$ the difference between the asteroid positions at $t_0 + \Delta T$ and with $\Delta\mathbf{v}'$ the difference between the asteroid velocities at the same epoch.

C. Phasing indicators as phasing value surrogates

The indicators introduced above may be used to rank transfer opportunities without having to compute the phasing value φ. In this sense, they act as surrogates to the phasing value and they will be valuable if the ranks obtained using them are correlated to those obtained using φ. In order to assess their quality we compute such a correlation using the Kendall-tau rank correlation coefficient. Consider two different rankings of possible transfer opportunities: $R_1 = [\mathcal{A}_{i_1}, .., \mathcal{A}_{i_n}]$ and $R_2 = [\mathcal{A}_{j_1}, .., \mathcal{A}_{j_n}]$, the Kendall-tau coefficient between two ranks is defined as:

$$\tau = 2\frac{n_c - n_d}{n(n-1)}$$

where n_c is the number of concordant pairs and n_d is the number of discordant pairs. Since the total number of pairs is $n(n-1)/2$, a value of $\tau = 1$ corresponds to two identical rankings, similarly a $\tau = -1$ corresponds to two perfectly discordant rankings and $\tau = 0$ represent a complete absence of correlation. As an example, consider the 16,256 asteroids of the main belt as defined in [10]. Select a random epoch t_0 and a random starting asteroid $\mathcal{A}_i$. Rank all transfer opportunities $\mathcal{A}_i$-$\mathcal{A}_j$, with $i \neq j$ at t_0 using the phasing value φ, the Euclidean indicator d_e, the orbital indicator d_o and the improved orbital indicator $d_{o'}$. To compute of φ use $\Delta T_M = 1$ [year] (we assume to be interested in transfer opportunities in a one year launch window) and $\alpha_M = 3.751 \cdot 10^{-4}$ [m/s^2]. Compute now the Kendall-tau coefficient over the first k asteroids and average over $N = 100$ distinct A_i, t_0 values. The results, shown in Fig.(2) show how the improved orbital metric outperforms all others in terms of showing a superior correlation to the ground truth. In particular, at low values of k, that is when we need to select only the best few options, the improved orbital indicator seems to be able to maintain a good correlation with the ground truth, while the euclidean distance and the orbital indicator fail to do so. In the same plot, the number of asteroids that are ranked within the first k positions according to the phasing value, but not according to an indicator, are also reported. Such a number is relevant when the indicators (or the phasing value) are to be used to prune out possible targets so that, for example, one can say that, on average, the improved orbital indicator leaves out of the first 100 selected targets 30 good options versus the 35 and 39 lost by respectively the orbital indicator and the euclidean indicator.

D. Use of the indicators

At any given epoch t_0 the set $\mathcal{A}$ of all asteroids is a metric space if any of the above indicators is introduced. This allows to define asteroid clusters and neighbourhoods and to compute them efficiently using well established methods. Take for example the problem of finding the k nearest neighbours with respect to one of the introduced indicators at t_0. In all three cases, given the low dimensionality of the k-NN problem, a k-d tree data structure [11] is an efficient choice to perform the computation. The complexity to build a static k-d tree is $O(N \log N)$, while the k-NN query has complexity $O(k \log N)$ where N would be the number of asteroids considered. One single k-NN query, including the construction of the k-d tree, on our test case that consider 16,256 main belt asteroids, takes 250 [ms] on average. This time can be

compared to the cost of computing the phasing value for all the asteroids which is 3 orders of magnitude higher. Such a remarkable difference is of particular importance, for example, in the context of search algorithm that have to build a long chain of possible visits where such a computation needs to be done frequently as to select the possible next transfer to branch towards [5].

III. Maximum initial mass - m^*

It is common, while performing the preliminary design of an interplanetary trajectory, to use a trajectory model based on ballistic arcs patched with impulsive manoeuvres in order to find low ΔV transfer options. This approach was also used in the previous sections, for example, to introduce the use or orbital indicators. Once a good opportunity is found using this approximation (called chemical propulsion model), the hope is that the resulting trajectory can be converted into a low-thrust trajectory where the impulsive manoeuvres are spread over a longer period of time. Such a conversion is often troublesome and the relation between the two models is complex and poorly understood. A frequent and common approach is to assume that a chemical propulsion leg of duration ΔT (for example a Lambert arc) and requiring some ΔV_L cannot be converted to low-thrust if:

$$\frac{T_{max}}{m}\Delta T \leq \Delta V_L \tag{4}$$

The reasoning being that if a spacecraft having mass m and thrusting at full magnitude for a duration ΔT, is unable (neglecting gravity) to build up the chemically required ΔV_L, there is little hope it will be able to make the transfer in the requested time using a low-thrust propulsion system. One can then derive, according to this simplification, an expression to approximate the maximum initial mass m^* that the spacecraft can have at the beginning of a trajectory leg in order for a given transfer to be feasible in low-thrust:

$$m^*_L = \frac{\Delta T}{\Delta V_L} T_{max} \tag{5}$$

Note that the maximum initial mass trajectory corresponds to a thrust structure that does not contain any coast arc (if it did it would be possible to increase the starting mass, which contradicts the optimality of m^*).

In the next section we introduce a new algebraic expression approximating the maximum initial mass m^* improving, in our test cases, by one order of magnitude the average error with respect to the commonly used approximation above.

A. The MIMA: maximum initial mass approximation

Consider a rendezvous trajectory from one starting asteroid $\mathcal{A}_1$ to a target asteroid $\mathcal{A}_2$. The starting and arrival epochs are denoted with t_s and t_t. The Lambert transfer between the two asteroids is easily computed from $\mathbf{r}_1(t_s)$, $\mathbf{r}_2(t_t)$ and from the transfer time $\Delta T = t_t - t_s$. Denote with $\mathbf{r}_L(t), \mathbf{v}_L(t)$ the position and velocity vectors along such a Lambert transfer and consider a non-rotating reference frame $\mathcal{F}$ attached to it. Consider now a spacecraft equipped with low-thrust propulsion and having to transfer between the same two asteroids (rendezvous conditions) and study its motion in the free falling $\mathcal{F}$ frame, neglecting all tidal effects of gravity. For comparison, these would result in an extra acceleration of the order of $3 \cdot 10^{-5}$ [m / s^2] at a distance 2.6 [AU] on a spacecraft offset by 0.1 [AU] from the origin. The equations of motion for the spacecraft are thus considered in their most simple form: $m\mathbf{a} = \mathbf{u}$, $\dot{m} = -\frac{u}{I_{sp} g_0}$. Assume now that, along the transfer, the spacecraft engines provide a constant acceleration $\mathbf{a}_1 = \frac{\mathbf{u}_1}{m}$ for a time $\tau \Delta T$, where $\tau \in [0, 1]$, and a constant acceleration $\mathbf{a}_2 = \frac{\mathbf{u}_2}{m}$ for the remaining time $(1-\tau)\Delta T$. We may then write:

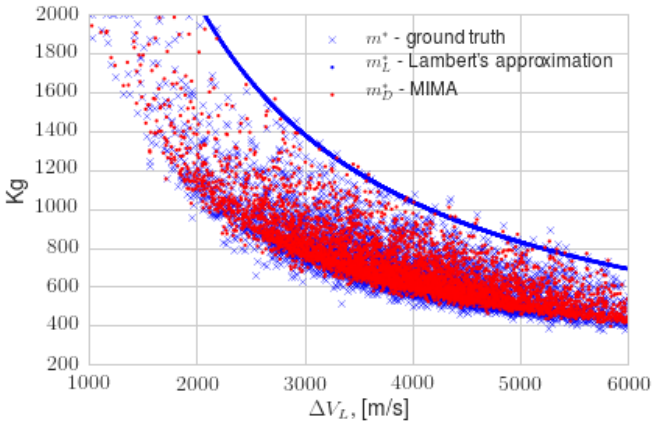

Fig. 3. The maximal initial mass m^* as computed from the Lambert model, from the new MIMA and compared to the ground truth. The RMSE of the Lambert's approximation is 477 [Kg] while the one relative to the proposed MIMA is 26.4 [Kg] (both computed considering only $m^* \in [500, 2000]$)

$$\begin{cases} \frac{\mathbf{v}_{\infty 1} - \mathbf{v}_{\infty 2}}{\Delta T} + \mathbf{a}_1 \tau + \mathbf{a}_2 (1-\tau) = \mathbf{0} \\ \frac{2\mathbf{v}_{\infty 1}}{\Delta T} + \mathbf{a}_1 \tau (2-\tau) + \mathbf{a}_2 (1-\tau)^2 = \mathbf{0} \end{cases} \tag{6}$$

which represent, in $\mathcal{F}$, the rendezvous conditions between the spacecraft and the target asteroid and where we have introduced the symbols $\mathbf{v}_{\infty 1} = \mathbf{v}_1(t_s) - \mathbf{v}_L(t_s)$ and $\mathbf{v}_{\infty 2} = \mathbf{v}_1(t_t) - \mathbf{v}_L(t_t)$ to denote the relative velocities between the spacecraft and the Lambert solution at departure and arrival. Under the further assumption $|\mathbf{a}_1| = |\mathbf{a}_2|$ it is possible to solve the above equations for $\tau, \mathbf{a}_1$ and $\mathbf{a}_2$, obtaining (see Appendix):

$$\begin{cases} \Delta T \tau \mathbf{a}_1 = (\mathbf{v}_{\infty 2} - \mathbf{v}_{\infty 1})\tau - (\mathbf{v}_{\infty 2} + \mathbf{v}_{\infty 1}) \\ \Delta T (\tau - 1)\mathbf{a}_2 = 2\mathbf{v}_{\infty 2} - (\mathbf{v}_{\infty 2} - \mathbf{v}_{\infty 1})\tau \\ \tau = \frac{\alpha + 1 - \text{sgn}(\alpha)\sqrt{1+\alpha^2}}{2} \end{cases} \tag{7}$$

where $\alpha = \frac{(\mathbf{v}_{\infty 2} + \mathbf{v}_{\infty 1}) \cdot (\mathbf{v}_{\infty 2} + \mathbf{v}_{\infty 1})}{(\mathbf{v}_{\infty 2} + \mathbf{v}_{\infty 1}) \cdot (\mathbf{v}_{\infty 2} - \mathbf{v}_{\infty 1})}$. These equations allow to find the accelerations $\mathbf{a}_1$ and $\mathbf{a}_2$, their magnitude a_D and the switch time τ from, essentially, the corresponding Lambert solution. The corresponding transfer is idealized and unpractical but it represents, in many cases, a good approximation to the zero-coast optimal solution: the solution to the fixed time optimal control problem where rather than minimizing the total mass of propellant used from a given initial spacecraft mass and thrust, we set to maximize the initial spacecraft mass, thus obtaining a trajectory that will not have any coast arc. Such a maximum initial mass m^* can thus be approximated considering a_D as the average acceleration along the trajectory, so that:

$$\begin{aligned} \frac{m^*_D + m_f}{2} &= \frac{T_{max}}{a_D} \\ m_f &= m^*_D \exp\left(\frac{-\Delta V_D}{I_{sp} g_0}\right) \end{aligned}$$

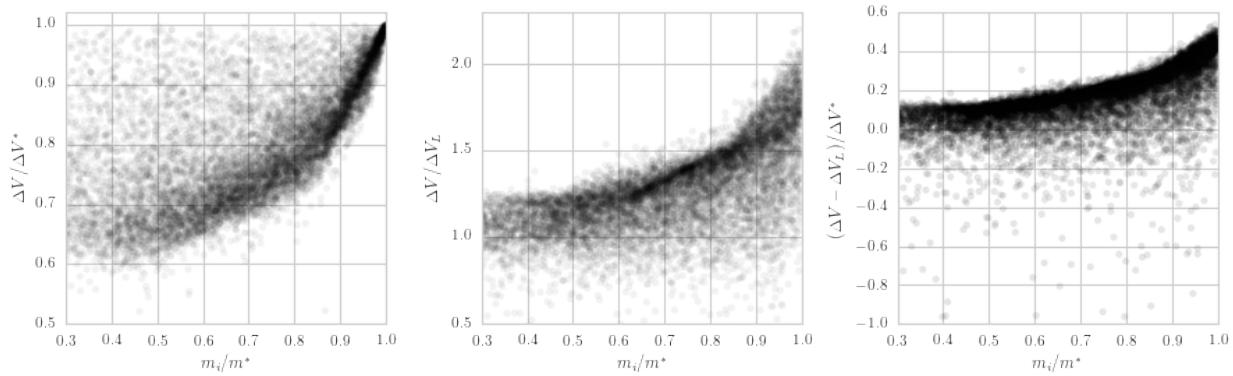

Fig. 4. Visualization of all training data (each point represents a mass optimal low-thrust trajectory)

TABLE I. VALUES USED TO CREATE THE REFERENCE DATABASE OF LOW-THRUST ARCS

variable	lower bound	upper bound	units
Neighbour	1	10	
t_1	9000	12000	MJD2000
T	100	420	days
m_i	$0.3m^*$	m^*	Kg

where $\Delta V_D = a_D \Delta T$. Solving for m_D^* we have:

$$m_D^* = 2\frac{T_{max}}{a_D}\left(1 + \exp\left(\frac{-a_D \Delta T}{I_{sp} g_0}\right)\right)^{-1} \tag{8}$$

which represents a remarkably simple algebraic expression relating the ΔV computed using a chemical model of an asteroid to asteroid transfer and the maximum initial mass that a spacecraft can have in order to be able to actually perform such a hop using its own low-thrust propulsion engines. Note that the computational complexity of the expression above is comparable to that of the Lambert approximation in Eq.(5) and it is that of solving one single zero-revolutions Lambert problem. We call this approximation the Maximum Initial Mass Approximation (MIMA).

1) Comparing m^*, m_L^* and m_D^*: In order to assess the error introduced by the approximate expressions in Eq.(5) and Eq.(8), we first compute the ground truth m^* by solving the full optimal control problem of a fixed time, asteroid to asteroid transfer, maximizing the initial starting mass. We do so for 10,000 randomly selected epochs t_s, asteroids $\mathcal{A}_1$-$\mathcal{A}_2$ and transfer times, taking care that $\mathcal{A}_2$ is within the best $k = 100$ candidates for a transfer from $\mathcal{A}_1$ at t_s according to the improved orbital metric with $\Delta T = 180$ [days]. We consider a spacecraft having a propulsion system capable of delivering $T_{max} = 0.3$ [N] continuously and a specific impulse of $I_{sp} = 3000$ [sec]. For each transfer we compute also the Lambert approximation m_L^* from Eq.(5) and the newly proposed expression m_D^* from Eq.(8). The results are visualized in Figure 3. Computing the mean absolute error (MAE) we get 430 [Kg] for the Lambert approximation and 20 [Kg] for the MIMA.

IV. LEARNING THE MAXIMUM FINAL MASS

Let us consider again a fixed time transfer between two asteroids $\mathcal{A}_1$ and $\mathcal{A}_2$. The corresponding trajectory, if $m_i = m^*$, will not have any coast arc and is well approximated by the MIMA. In general, though, one may want to predict what happens in cases where $m_i < m^*$, which will result in the presence of a coast arc. In particular one would want to predict m_f, i.e. the optimal final mass of the spacecraft, without having to solve the corresponding maximum mass optimal control problem. A first, crude, approximation often made in preliminary stages of trajectory design is based on the assumption that the overall ΔV required is that of a Lambert transfer, hence:

$$m_{f_L} = m_i\left(1 - \exp\frac{-\Delta V_L}{I_{sp} g_0}\right) \tag{9}$$

Here we propose to use machine learning techniques to find a better estimate. Our approach improves greatly on the naive formula above, at the cost of creating a database of reference solutions to learn from (the supervised signal).

A. The database of low-thrust trajectories

Consider the same reference spacecraft used above. Choose an asteroid $\mathcal{A}_1$ at random from the reference main belt population defined in [10] and a second asteroid $\mathcal{A}_2$ chosen at random from $\mathcal{A}_1$ closest $k = 10$ neighbours as defined by the improved orbital indicator. Consider a random starting epoch $t_1 \in [9000, 12000]$ [MJD2000] and a random transfer time $T \in [100, 420]$ [days]. Solve the optimal control problem of maximum initial mass to find m^*. Consider then a random initial mass $m_i \in [0.3, 1]m^*$ [Kg] and solve the maximum final mass optimal control problem transferring the spacecraft (rendezvous conditions) from $\mathcal{A}_1$ to $\mathcal{A}_2$. Repeating this procedure 100,000 times, recording the obtained optimal final mass m_f, results in a large database of optimal low-thrust legs.

In Figure 4 we visualize all trajectories in the database. On the abscissa we report the quantity m_i/m^* which, necessarily, is such that $0.3 < m_i/m^* < 1$, while on the ordinate we show three different quantities. First (on the left plot) we report the ratio $\Delta V/\Delta V^*$ between the ΔV accumulated along the optimal trajectory and along the maximum initial mass trajectory. Such a ratio appears to always be smaller than one, a conjecture that has an immediate implication on the coast arc duration ΔT_c:

$$\Delta T_c \geq \Delta T\left(1 - \frac{m_i}{m^*}\right),$$

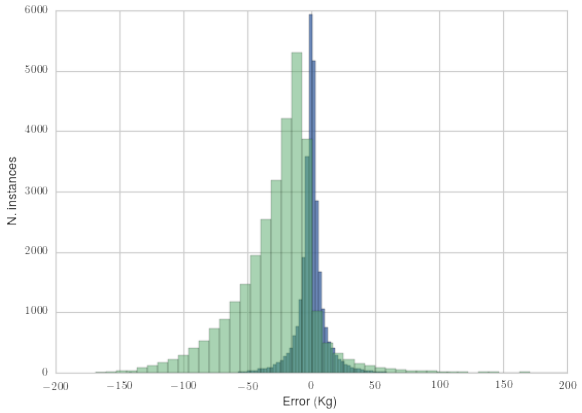

Fig. 5. Absolute error distribution on the test set using the Lambert model (green) or the gradient boosting regressor (blue)

deriving from the relations $\Delta V = v_e \log(m_i/m_f)$ and $\Delta V^* = v_e \log(m^*/m_f^*)$, since $m_f^* = m^* - c\Delta T$ and $m_f = m_i - c[\Delta T - \Delta T_c]$. Most notably, this ratio appears to be mainly clustered in a narrow area of the plot (the darker region) highlighting the correlation between the length of the resulting coast arc and the ratio m_i/m^*. In the second plot (center) we report the ratio $\Delta V/\Delta V_L$ between the ΔV accumulated along the optimal trajectory and that computed from a pure Lambert transfer. We observe, again correlated data points. Most points are such that $\Delta V > \Delta V_L$, corresponding to the fact the majority of the Lambert transfers are, in this case, actually using the optimal number of impulses (two) and they are thus an optimal strategy. Some data point, though, have a $\Delta V < \Delta V_L$ which correspond to those cases where the Lambert two impulse transfer could be improved by adding more impulses along the way, a strategy that is better approximated by the low-thrust profile. We also report, in the third plot, the ratio between the ΔV difference between the optimal and the Lambert solution and ΔV^*, which shows a clear correlation.

B. The attributes

In order to learn the optimal final mass m_f of a low-thrust transfer (of the spacecraft $\mathcal{S}$) defined by the transfer time T, the initial mass m_i, the starting state $\mathbf{r}_1$, $\mathbf{v}_1$ and the end state $\mathbf{r}_2$, $\mathbf{v}_2$, we consider the following attributes that can be computed at the cost of one Lambert's problem solution and some added trigonometry: ΔT, m_i, m_D^*, m_L^*, ΔV_D, ΔV_L, $\cos\theta$, n_1, n_2, $\Delta\mathbf{r}$, $\Delta\mathbf{v}$. Table II describes each attribute in more details. The attributes were "manually" selected using the domain knowledge we possess on the problem. Some trial and error attempts were made to remove or add attributes and it was noted how, while all important to some extent, it is m_D^* to carry, by large, the most information on the predicted m_f value. Thus, to confirm and study its relevance, the ground truth value m^* was used instead in some separate trials noting how it allowed some regressors to reach a MAE smaller than 3 [Kg] and confirming the importance of the maximum initial mass to predict m_f.

TABLE II. ATTRIBUTES CONSIDERED TO LEARN m_f

attribute	explanation
ΔT	Transfer time
m_i	Initial spacecraft mass
m_D^*	MIMA
m_L^*	Maximum initial mass computed using the Lambert transfer
ΔV_D	ΔV approximated using the MIMA
ΔV_L	ΔV of the Lambert transfer
$\cos\theta$	Cosine of the inclination between starting and arrival orbit
n_1, n_2	Mean motion of the starting and arrival orbit
$\Delta\mathbf{r}$	Difference between the starting and arrival position vectors
$\Delta\mathbf{v}$	Difference between the starting and arrival velocity vectors

TABLE III. PERFORMANCE OF REGRESSORS

Regressor	MAE [Kg]	RSME [Kg]	CPU time [s] (training)
Lambert's predictor	31.44	42.77	
Random Forest	8.64	13.88	4.16
Bagging	8.64	13.81	4.21
AdaBoost	24.6	30.4	6.18
Extra Forest	8.56	13.77	1.34
Gradient Boosting	**7.86**	**12.48**	24.81
Decision Tree	12.33	19.21	0.73
Extra Tree	13.47	20.99	0.12

C. Results from different regressors

We divide our database in a data set containing 70,000 trajectories and a test set containing the remaining 30,000. As a reference, we first evaluate the mean average error (MAE) and the root square mean error (RSME) using the Lambert model as a predictor for the fianl mass, i.e. Eq.(9). We then train a number of different state-of-the art regressors and record for each of them the MAE and the RSME. The implementation we used of all the regressors is taken from scikit-learn, a popular scientific toolbox for Machine Learning. The parameter chosen for each algorithm are the default choices, except for gradient boosting where a maximum depth of 7 was used instead of the default value as it was noted how the performances are extremely sensitive to this parameter. For the same reason, for AdaBoost, the loss was set to be of the squared type and 100 estimators and a learning rate of 1.5 were used. For ensemble type of regressors, decision trees are used as the base estimator.

The results are summarized in Table III. We do not here present a thorough analysis on the performance (and chosen parameters) for of all these machine learning techniques as it here suffices to note how they all improve considerably over the Lambert's predictor and that they provide a rich portfolio of choices both for CPU time and performances. Clearly, tuning the parameters and the details of each single method, or including more state of the art approaches would be likely to improve the results even further. The detailed study on the use of modern machine learning techniques for this case study will be the subject of a future publication.

In Figure 5 we visualize the distribution, across the test set, of the absolute error in the case of the use of a Lambert's model and of the best learned model, the one from the gradient boosting regressor. We note how most data points are within a very small error. The maximum absolute error is also contained by the use of the learned model, while the distribution relative to the Lambert's model has longer tails with some notable trajectories being completely misrepresented being the maximum error $\epsilon = 643$ [kg] against $\epsilon = 143$ [Kg] of the best regressor.

V. Conclusions

In this paper we propose and test a number of fast approximators of important quantities characterising mass optimal low-thrust transfers between main-belt asteroids. In particular we approximate the phasing value φ (describing the neighbourhood of an asteroid intended as the set of reachable asteroids), the maximum initial mass m^* (defining the upper bound on the spacecraft mass in order for a target asteroid to be reachable) and the maximum final mass m_f (defining the optimal value of the spacecraft mass at any target asteroid). We find that the proposed approximations all represent a distinct improvement in terms of computational time over the state of the art methods able to compute the ground truth. The approximators are found to be a distinct improvement in terms of precision over the Lambert's model approximation, while using comparable computational time. In the case of the final mass approximator, we introduce the idea of learning from a large database of optimal solutions. Our result open the possibility to build more efficient and reliable searches on the combinatorial part of preliminary interplanetary trajectories design for the asteroid belt exploration.

Appendix
Proof of Eq. 7

Introduce the variables $\mathbf{A} = \Delta T \mathbf{a}_1 \tau$, $\mathbf{B} = \Delta T \mathbf{a}_2 (1-\tau)$, $\mathbf{V} = \mathbf{v}_{\infty 2} - \mathbf{v}_{\infty 1}$ and $\mathbf{U} = \mathbf{v}_{\infty 2} + \mathbf{v}_{\infty 1}$. We can write Eq.(6) in terms of the new quantities as:

$$\begin{cases} -\mathbf{V} + \mathbf{A} + \mathbf{B} = \mathbf{0} \\ \mathbf{U} - \mathbf{V} + \mathbf{A}(2-\tau) + \mathbf{B}(1-\tau) = \mathbf{0} \end{cases}$$

and, solving for $\mathbf{A}$ and $\mathbf{B}$ we get:

$$\begin{cases} \mathbf{A} = \mathbf{V}\tau - \mathbf{U} \\ \mathbf{B} = \mathbf{V}(1-\tau) + \mathbf{U} \end{cases} \tag{10}$$

Squaring the formulas above, we have also:

$$\begin{cases} \Delta T^2 a_1^2 = V^2 + \frac{U^2}{\tau^2} - 2\frac{\mathbf{U}\cdot\mathbf{V}}{\tau} \\ \Delta T^2 a_2^2 = V^2 + \frac{U^2}{(1-\tau)^2} + 2\frac{\mathbf{U}\cdot\mathbf{V}}{1-\tau} \end{cases}$$

Introducing the condition $a_1 = a_2$ the above equations can equated and solved for τ:

$$2\tau^2 - 2\tau(\alpha+1) + \alpha = 0$$

where $\alpha = \frac{U^2}{\mathbf{U}\cdot\mathbf{V}}$. Solving the quadratic expression above and accounting for the fact that $\tau \in [0,1]$ we get:

$$\tau = \frac{\alpha + 1 - \mathrm{sgn}(\alpha)\sqrt{1+\alpha^2}}{2} \tag{11}$$

Substituting again in Eq.(10) and Eq.(11) the definitions of $\mathbf{A}$, $\mathbf{B}$, $\mathbf{U}$ and $\mathbf{V}$ we obtain Eq.(7).

References

[1] European Space Agency. GTOC portal. [Online]. Available: http://sophia.estec.esa.int/gtoc_portal

[2] D. Izzo, L. F. Simões, M. Märtens, G. C. De Croon, A. Heritier, and C. H. Yam, "Search for a grand tour of the jupiter galilean moons," in *Proceedings of the 15th annual conference on Genetic and evolutionary computation*. ACM, 2013, pp. 1301–1308.

[3] T. N. Edelbaum, "Propulsion requirements for controllable satellites," *ARS Journal*, vol. 31, no. 8, pp. 1079–1089, 1961.

[4] A. E. Petropoulos and J. M. Longuski, "Shape-based algorithm for the automated design of low-thrust, gravity assist trajectories," *Journal of Spacecraft and Rockets*, vol. 41, no. 5, pp. 787–796, 2004.

[5] D. Izzo, D. Hennes, L. F. Simões, and M. Märtens, "Designing complex interplanetary trajectories for the global trajectory optimization competitions," in *Space Engineering: Modeling and Optimization with Case Studies*, ser. Springer Optimization and Its Applications, G. Fasano and J. D. Pintér, Eds. Springer, 2016.

[6] Z. Michalewicz, "A survey of constraint handling techniques in evolutionary computation methods." *Evolutionary Programming*, vol. 4, pp. 135–155, 1995.

[7] Q. Zhang and H. Li, "MOEA/D: A multiobjective evolutionary algorithm based on decomposition," *Evolutionary Computation, IEEE Transactions on*, vol. 11, no. 6, pp. 712–731, 2007.

[8] A. Mambrini and D. Izzo, "PaDe: a parallel decomposition algorithm based on the MOEA/D framework and the island model," in *Parallel Problem Solving from Nature–PPSN XIII*. Springer, 2014, pp. 711–720.

[9] K. Nowak, M. Märtens, and D. Izzo, "Empirical performance of the approximation of the least hypervolume contributor," in *Parallel Problem Solving from Nature–PPSN XIII*. Springer, 2014, pp. 662–671.

[10] L. Casalino and G. Colasurdo, "Problem Description for the 7th Global Trajectory Optimisation Competition," 2014, [Online; accessed 10-March-2016].

[11] J. L. Bentley, "Multidimensional binary search trees used for associative searching," *Commun. ACM*, vol. 18, no. 9, pp. 509–517, Sep. 1975.